Neutron diffraction study of the magnetic ordering in the $Ho(Mn_{1-x}Al_x)_2$ system

1998 J. Phys.: Condens. Matter 10 11755

(http://iopscience.iop.org/0953-8984/10/50/014)

J. Phys.: Condens. Matter **10** (1998) 11755–11764. Printed in the UK PII: S0953-8984(98)96276-2

Neutron diffraction study of the magnetic ordering in the $Ho(Mn_{1-x}Al_x)_2$ system

I S Dubenko†, I V Golosovsky‡¶, A S Markosyan§ and I Mirebeau‖

† Institute of Radioengineering, Electronics and Automation, 117454 Moscow, Russia
‡ St Petersburg Nuclear Physics Institute, 188350 Gatchina, St Petersburg, Russia
§ Faculty of Physics, M V Lomonosov Moscow State University, 119899 Moscow, Russia
‖ Leon Brillouin Laboratory, CE-Saclay, F-91191 Gif-sur-Yvette Cédex, France

Received 24 July 1998, in final form 7 October 1998

Abstract. The magnetic and crystal structure of the as-cast cubic $Ho(Mn_{1-x}Al_x)_2$ compounds ($x \leqslant 0.1$) was studied using neutron powder diffraction. The samples showed substantial inhomogeneity and consisted of at least two C15-type crystal phases. In the first phase predominating in $HoMn_2$ (96.3%) ferrimagnetic long range order is stable. The second phase with the cell parameter lying within the narrow range 7.49–7.52 Å shows an incommensurate magnetic structure with a wave vector $\boldsymbol{k} \approx [0.18, 0.18, 0.08]$ weakly dependent on x. Short range correlations of an antiferromagnetic type along with long range ordering were observed. The diffuse maxima lie at the positions corresponding to the Bragg reflections with half-integer indices and are ascribed to short range correlations based on the MnO-type antiferromagnetic structure developed within clusters of ∼25 Å in size. No volume effect associated with the onset of Mn magnetism was observed up to $x = 0.1$.

1. Introduction

The RMn_2 (where R is rare earth element) compounds with the Laves phase structures are characterized by an instability of Mn magnetism in a highly frustrated structure. The instability was accounted for by the existence of a critical Mn–Mn nearest-neighbour distance ≈2.68 Å corresponding to the lattice parameter $a_c \approx 7.62$ Å, above which the Mn subsystem exhibits a sudden ordering at low temperatures in the compounds with R = Y, Sm, Pr, Nd, Gd and Tb [1]. This concept was confirmed qualitatively by numerous experiments with substituted $(R, R')Mn_2$ or $R(Mn, Me)_2$ (Me: metal) systems and measurements under external pressure [2–6]. Some authors emphasized the importance of the magnetic field in stabilizing Mn magnetism [7, 8]. In $TbMn_2$, the lattice parameter of which is close to a_c, the Mn sublattice can be demagnetized by applying an external magnetic field [7]. It is accepted that the strength of the f–d interaction varies in the same way throughout the RMn_2 series as the lattice parameter (Mn–Mn distance). Hence, at least two factors can be responsible for Mn moment formation in these compounds. Application of simple models for interpreting the nature of Mn magnetism in the RMn_2 compounds is therefore questionable.

It is assumed that the Mn sublattice can exist in two different states: a transformed phase (TP) with large local magnetic moments of about 2.6 μ_B at the Mn sites and a

¶ Address for correspondence: Dr I V Golosovsky, St Petersburg Nuclear Physics Institute, 188350 Gatchina, St Petersburg, Russia. E-mail address: golosov@hep486.pnpi.spb.ru.

0953-8984/98/5011755+10$19.50

non-transformed phase (NTP) with induced Mn moments continuously varying between 0 and ∼1.5 μ_B [5, 6]. In the TP the Mn subsystem shows a huge positive volume effect (∼10^{-2}), associated with the appearance of an intrinsic Mn magnetic moment, while no volume expansion was observed in NTP. In [9] it was suggested that the transition between the magnetic and non-magnetic states of Mn has non-magnetic origin and can be treated as a kind of first order structural phase transition, which induces then a magnetic transition. The authors of [10] suggested a diffusionless phase transformation in order to account for the properties of the TP–NTP transition in the Mn subsystem.

Considering the magnetic spin arrangement, a number of complex magnetic structures was observed by neutron diffraction experiments in RMn_2 and $(R, Y)Mn_2$ compounds with R = Tb, Dy and Ho when the Mn sublattice is still in the NTP [6, 11–17]. In fact, three types of antiferromagnetic ordering known for the f.c.c. lattice were found in the NTP, which can coexist with a ferromagnetic ordering. In the $Tb_{1-x}Y_xMn_2$, $Ho_{1-x}Y_xMn_2$ and $Dy_{1-x}Y_xMn_2$ systems a coexistence of short range order with the long range AF2 (MnO)-type magnetic structure was observed [6, 16, 18].

The magnetic structure both of cubic and hexagonal $HoMn_2$ has been investigated by several authors. According to the early neutron diffraction experiments a ferrimagnetic structure with $T_N = 26$ K was proposed; no additional lines except those allowed for the f.c.c. lattice were detected [12]. However, the neutron diffraction patterns of the cubic $HoMn_2$ samples studied in [11, 14] showed reflections with half-integer indices corresponding to a magnetic cell doubled in all three directions. It was shown that the arrangement of the Ho magnetic moments has both antiferromagnetic and ferromagnetic components, while the Mn spins are ordered antiferromagnetically. The most prominent result of that work was that the Mn magnetic moments of 0.6(2) μ_B were induced at every fourth crystallographic site only, between the (111)-planes of the Ho atoms in a strongly polarizing environment. This magnetic structure is similar to the structure observed in $DyMn_2$ [13], $TbMn_2$ (NTP) and $Tb(Mn_{0.96}Fe_{0.04})_2$ [6, 15].

A regular change of the interatomic Mn–Mn spacing can be realized by Mn substitutions, which give rise to a drastic change in the basic magnetic properties. The NMR and thermal expansion measurements of the $Y(Mn_{1-x}Me_x)_2$ systems where Me = Al (a increasing with x) [19] and Fe, Co (a decreasing with x) [2] have shown that Al suppresses the appearance of TP at higher concentration compared to the case of Fe or Co due to the essential increase of the lattice parameter. On the other hand, the TP of Mn does not appear in the $Ho(Mn_{1-x}Al_x)_2$ system at least up to $x = 0.2$ [3]. Nevertheless, the temperature behaviour of the low field susceptibility indicates that the magnetic structure of this system in the NTP could be dependent on substitutions. The purpose of this work is to study the magnetic structures arising in the cubic $Ho(Mn_{1-x}Al_x)_2$ system at small Al substitutions $x = 0.0$; 0.05; 0.1 and compare them with those observed in other RMn_2 intermetallics.

2. Sample preparation and experimental details

Polycrystalline samples of the $Ho(Mn_{1-x}Al_x)_2$ compounds with $x = 0$; 0.05 and 0.1 were synthesized by induction melting under protective argon atmosphere in a water-cooled copper crucible. The purity of the raw materials was 99.9% (Ho), 99.9% (Mn) and 99.99% (Al). The initial stoichiometry was chosen as 1:1.92 for all the samples to prevent the appearance of foreign phases. $HoMn_2$ is known to crystallize in the hexagonal C14-type Laves phase structure provided the ingots are cooled down slowly after the high temperature heat treatment. The preparation of the cubic samples with the C15-type crystal structure

needs quenching. In order to stabilize the C15-type structure, the ingots were quickly cooled down in the crucible by switching off abruptly the heating power. Hence, as-cast samples were used in the experiments.

The neutron diffraction measurements were carried out at the multicounter diffractometer of St Petersburg Institute of Nuclear Physics using a neutron wavelength of 1.655 Å. The diffractometer G6-1 of the Laboratory of Leon Brillouin with a large neutron wavelength of 4.732 Å was used for the search of long period structures. All the neutron diffraction patterns were treated by the program FULLPROF [20].

3. Experimental results

3.1. Magnetic scattering at low temperatures

In figure 1 the neutron diffraction patterns are shown of the $Ho(Mn_{1-x}Al_x)_2$ samples collected at the lowest temperature 8 K together with the pattern for $Ho(Mn_{0.9}Al_{0.1})_2$ measured in the paramagnetic phase at 140 K. Instead of well defined superstructure Bragg reflections with half-integer indices observed in [14] only broad maxima appear at their positions. The intensity of these diffuse 'reflections' increases with increasing of Al concentration. In addition to the diffuse magnetic scattering, a ferromagnetic contribution to the nuclear reflections is also present. From the temperature dependence of the ferromagnetic component the magnetic ordering temperature T_C was evaluated. For $HoMn_2$ the value of $T_C = 25$ K is close to that reported previously [11, 12, 14] and increases slightly up to 30 K in $Ho(Mn_{0.9}Al_{0.1})_2$ (figure 2(a)).

Besides the diffuse magnetic scattering and ferromagnetic contribution, some superstructure reflections resulting from a long period incommensurate structure were also observed. A peak marked hereafter as a 'zero' satellite can clearly be seen in all the patterns given in figure 1. This peak corresponds to a periodicity of about 28 Å. In $Ho(Mn_{0.9}Al_{0.1})_2$ additionally two weak satellite reflections are observable. In figure 1(c) they are marked as 'A' and 'B'. The reflection marked by an asterisk does not change with temperature and is referred to an unidentified contamination. It is then omitted below from the patterns for the sake of simplicity.

The superstructure satellites found in the $Ho(Mn_{1-x}Al_x)_2$ system still persist far above T_C. They disappear at about 120 K in $Ho(Mn_{0.9}Al_{0.1})_2$ and at 100 K in $HoMn_2$ (figure 2(c)). The temperature dependence of the satellite positions is shown in figure 3. As can be seen, the wave vector of the incommensurate magnetic phase 'locks in' below T_C. Furthermore, a visible change in the temperature dependence of the full width at half maximum (FWHM) of the zero satellite can be detected at T_C (figure 4). Note that any associated magnetovolume effect, which could be referred to the onset of Mn magnetism, was not detected around these temperatures.

Since the satellite peaks and diffuse scattering are most developed in $Ho(Mn_{0.9}Al_{0.1})_2$, in the next section this compound will be discussed in more detail.

3.2. Magnetic and crystal structures of Ho($Mn_{0.9}Al_{0.1}$)$_2$

3.2.1. Incommensurate magnetic structure. As figure 3 shows above T_C the positions of satellites 'A' and 'B' move out in opposite directions when changing temperature, i.e. they give rise to nuclear nodes of the {220} type. A comparison with the calculated satellite positions shows that the incommensurate magnetic structure can well be described by a wave vector which is approximately directed along the $[\mu, \mu, 0]$ direction.

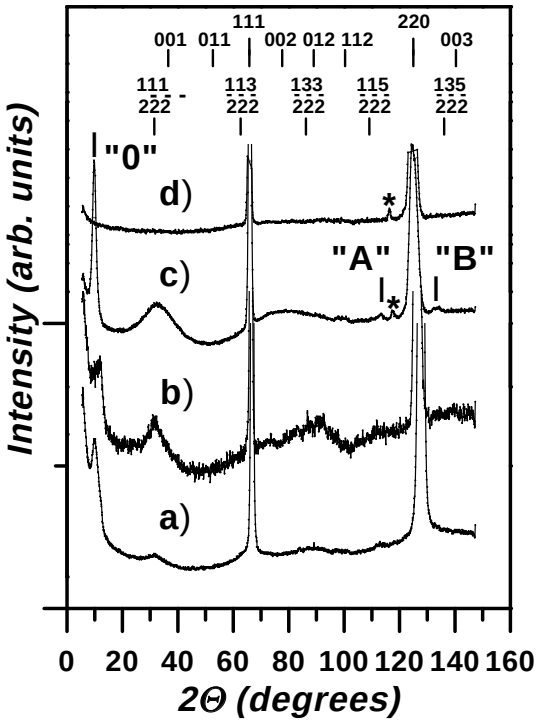

Figure 1. The neutron diffraction patterns of the $Ho(Mn_{1-x}Al_x)_2$ compounds with $x = 0.0$, 0.05 and 0.1 at 8 K (a, b, c) and $Ho(Mn_{0.9}Al_{0.1})_2$ at 140 K (d) measured at the neutron wavelength 4.76 Å. The positions of the nuclear Bragg reflections and those corresponding to the antiferromagnetic structure AF2 reported in [5] are marked by stripes at the top. The peaks marked as '0', 'A' and 'B' correspond to the incommensurate magnetic structure. The peak, marked by an asterisk corresponds to an unidentified impurity phase. All the profiles are normalized to the intensity of the nuclear reflections in order to reduce the patterns collected from different amount of sample to the same scale. The poor statistics for $Ho(Mn_{0.95}Al_{0.05})_2$ is due to the small amount of sample.

Since the wave vector $\boldsymbol{k}$ of the incommensurate structure does not change below T_C, all patterns of the $Ho(Mn_{0.9}Al_{0.1})_2$ sample measured below T_C are identical and can therefore be summed for further analysis. By fitting the resulting peak profiles by Gaussians the satellite positions were then determined with a precision not worse than 0.04° for satellites 'A' and 'B' and 0.01° for satellite '0'. In figure 5(a) the calculated satellite positions corresponding to all the {220} nodes of the $Ho(Mn_{0.9}Al_{0.1})_2$ sample for different lattice parameters a are shown by cross-mark branches. The position of the 220 nuclear reflection is shown by a filled-square branch. Each cross-mark branch corresponds to a definite nuclear node in the reciprocal space shown at the top of the figure.

The satellite pairs $(20\bar{2})^-$ and $(20\bar{2})^+$ (as well as $(02\bar{2})^-$ and $(02\bar{2})^+$ or $(2\bar{2}0)^-$ and $(2\bar{2}0)^+$) correspond to the wave vectors $\boldsymbol{k}$ and $-\boldsymbol{k}$, therefore their intensities should be practically equal. As seen, the satellite originating from the 220 nuclear node and marked 220^- in figure 5(a) is absent in the neutron diffraction pattern. Following the basic formalism, the magnetic scattering along this direction is absent if its diffraction vector $\boldsymbol{q}$ coincides with the direction of the magnetic moments. Suppose that $\boldsymbol{k} = [\mu, \mu, \nu]$, where μ and ν are small values. Hence, the absence of the 220^- satellite with $\boldsymbol{q} = [2-\mu, 2-\mu, -\nu]$

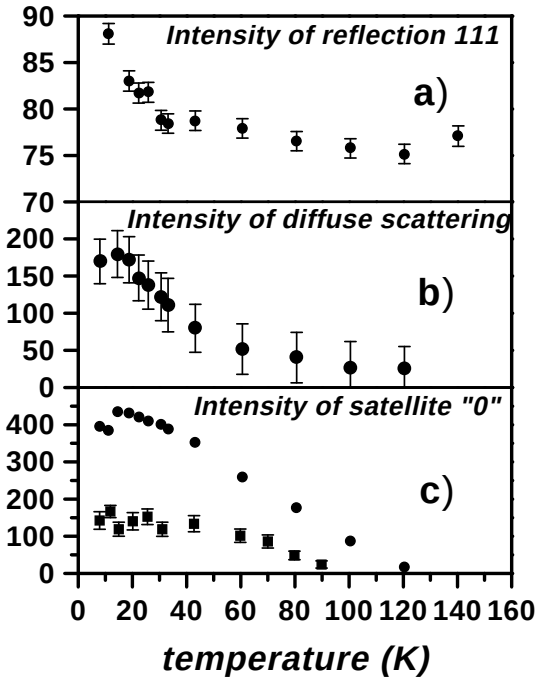

Figure 2. The temperature dependence of the magnetic scattering of the $Ho(Mn_{0.9}Al_{0.1})_2$ sample: (a) total intensity of the 111 magnetic contribution; (b) total intensity of the diffuse scattering; (c) intensity of the superstructure '0' satellite for $x = 0.1$ (the error bars are smaller than the symbol size) and for $HoMn_2$ (full squares). All intensities are in arbitrary units.

can be understood assuming that the magnetic component related to the incommensurate structure *is aligned close* to the [1, 1, 0] direction. Then, if $\boldsymbol{k} = [\mu, \mu, 0]$, the zero satellite, the scattering vector of which is directed exactly along $\boldsymbol{k}$, should vanish. Hence, the wave vector $\boldsymbol{k}$ must have a z-component, i.e., $\boldsymbol{k} = [\mu, \mu, \nu]$. In reality, the best agreement between the calculated and observed satellite positions was obtained by least squares refinement with the wave vector components μ and ν equal to 0.1799(3) and 0.0813(7), respectively, and the lattice parameter equal to 7.5173(6) Å. Note that an incommensurate magnetic structure with a similar wave vector $\boldsymbol{k} = [\mu, \mu, 0]$ was reported for YMn_2 [21].

3.2.2. Heterogeneity. The nuclear reflections of $Ho(Mn_{0.9}Al_{0.1})_2$ are noticeably broadened compared to those of $HoMn_2$, which can partly be accounted for by the internal stresses induced by substitution of Al for Mn. Uniform internal stresses were also found to exist in the cubic $HoMn_2$ sample investigated in [14]. However, a close inspection of the nuclear profiles of the as-cast samples studied in this work revealed their pronounced asymmetry, which changes with temperature. Its character differs from the standard instrumental asymmetry connected with the finite size of the detector. The asymmetry of the 220 peak of $Ho(Mn_{0.9}Al_{0.1})_2$ at 8 K can be seen in figure 5.

The calculated positions of the nuclear 220 reflection of $Ho(Mn_{0.9}Al_{0.1})_2$ are shown in figure 5(a) by filled squares. They are shifted from the centre of the experimental peak to higher diffraction angles. Hence, there should be *at least two* unresolved reflections,

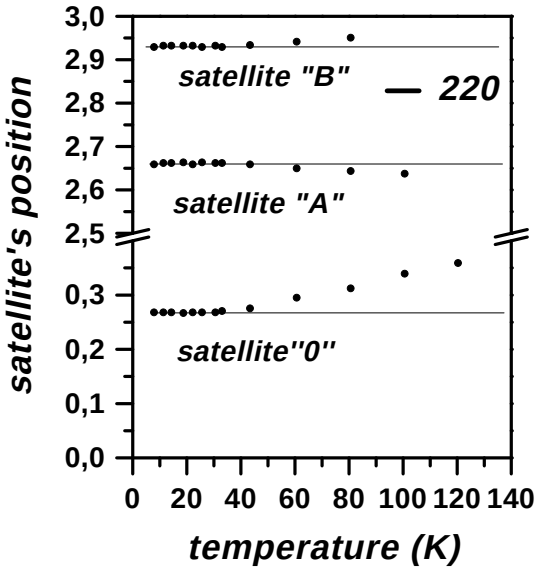

Figure 3. The temperature dependence of the satellite positions in q-space (in $2\pi/a$ units): $q = 4\pi \sin\vartheta/\lambda$ is the momentum transfer and a is the lattice parameter. The horizontal stripe corresponds to the 220 nuclear peak positions. The error bars are lower than the symbol size.

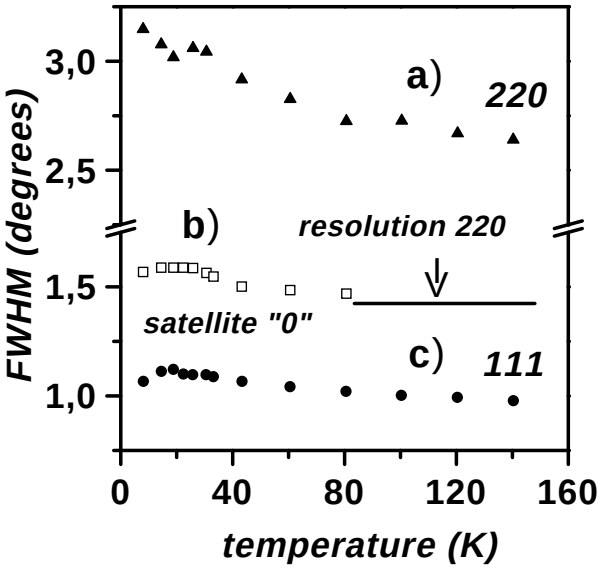

Figure 4. The temperature dependence of FWHM for the nuclear reflection 220 (a), the superstructure reflection marked in figure 1 as '0' (b) and the 111 reflection (c). The full line marked by an arrow corresponds to the instrumental resolution at the diffraction angle corresponding to the reflection 220.

and the incommensurate magnetic structure arises only in the phase with the smaller lattice parameter. In figure 5(b) the approximation of the resulting profile measured at 8 K is shown

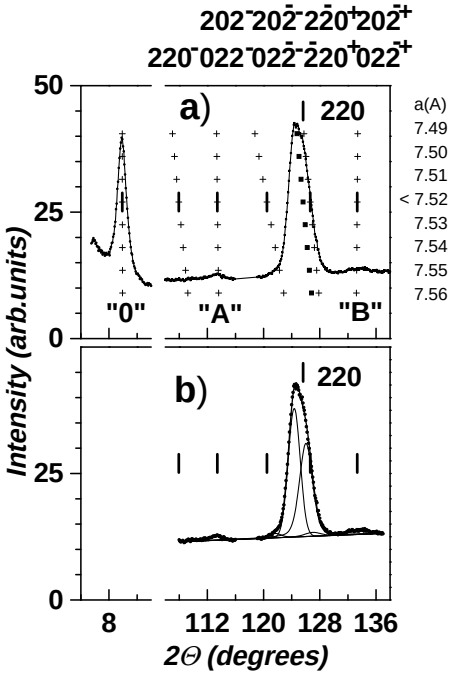

Figure 5. (a) The satellite positions of $Ho(Mn_{0.9}Al_{0.1})_2$ calculated by a least-squares method for different values of a. They are shown at the right-hand side of the diagram opposite to each set of crosses. Each branch of crosses corresponds to one of the {220}-type nodes in the reciprocal space (shown at the top of the figure), the branch of full squares corresponds to the 220 nuclear reflection. The vertical stripes indicate their positions for $a = 7.52$ Å. (b) Deconvolution of the 220 peak of $Ho(Mn_{0.9}Al_{0.1})_2$ measured at 8 K.

within the frame of the two-phase model. The refined FWHMs of both the reflections are very close to those found for $HoMn_2$. The volume content of each crystallographic phase in the sample of $Ho(Mn_{0.9}Al_{0.1})_2$, with the smaller and larger lattice parameter, has been estimated as 45.5% and 54.5%, respectively, from the measurements in the paramagnetic region at 140 K.

3.2.3. Ferrimagnetic ordering. According to the fitting procedure, the ferromagnetic contribution to the nuclear reflections is due to the usual collinear structure with the Ho and Mn moments coupled antiparallel. This structure is similar to that observed earlier in [12]. Substitution of Al for Mn leads to a drastic reduction of the Ho ferromagnetic component from 7 μ_B to about 2 μ_B in the $Ho(Mn_{0.9}Al_{0.1})_2$ sample, in agreement with the data reported in [3].

The magnetic contribution appears only at the reflections belonging to the larger lattice parameter crystal phase. It can therefore be concluded that the ferromagnetic and incommensurate structures do not coexist in the $Ho(Mn_{0.9}Al_{0.1})_2$ sample. In contrast, the observed phenomenon should be attributed to the coexistence of two crystallographic phases slightly different in their lattice parameters and having different magnetic structures.

3.2.4. Short range magnetic ordering. The diffuse scattering observed in $Ho(Mn_{0.9}Al_{0.1})_2$ can be considered as evoked by the basic structure of the AF2 type. This type of long

range order was observed in the cubic $HoMn_2$ sample studied in [14]. In the present work, assuming that the AF2 magnetic structure in the as-cast $Ho(Mn_{0.9}Al_{0.1})_2$ sample is developed within finite-size clusters, the profile analysis of the diffuse peaks was performed using a Thompson–Cox–Hastings pseudo-Voigt approximation for the line shape [22]. The analysis showed that the resulting fit could be improved substantially assuming a presence of extra 'diffuse reflections' with integer indices corresponding to a primitive cubic lattice. In figure 1 the 'diffuse reflections' 001 and 002 with maximal intensity can be distinguished. The refinement procedure gives a value of about 23–26 Å for the volume-averaged diameter of clusters, both AF2 type and those based on the primitive lattice. This value does not change with temperature. From the experimental data available we were not able to distinguish to what the crystal phase short range order should be attributed. The correlations can also be risen in both the phases simultaneously.

In the 'sandwich' model of the magnetic structure proposed for $DyMn_2$ [13], $HoMn_2$ [14] and $TbMn_2$ (NTP) [15] Mn has an induced moment only at the positions interposed between the 111 planes. For this model, the 1/2 1/2 3/2 and 1/2 1/2 1/2 reflections should have approximately equal intensities. However, as figure 1 shows, the 1/2 1/2 3/2 'diffuse reflection' in $Ho(Mn_{0.9}Al_{0.1})_2$ is strongly reduced (as well as the 111 'diffuse reflection' around the 111 nuclear reflection). This indicates that the observed short range correlations are mainly of antiferromagnetic nature, the ferromagnetic component being negligible. In fact, the refinement procedure carried out within the frame of the 'sandwich' model with the use of only half-integer indices gives Mn moment values exceeding any reasonable value. The best fit to observed intensities was obtained for the AF2 model; however each Mn atom should then be magnetic. Hence, the magnetic structure developed within the clusters differs from that observed in [14] for $HoMn_2$. The experimental data do not provide enough information to resolve unambiguously the magnetic structure associated with the 'diffuse reflections'. Due to the absence of the 011 'diffuse reflection' this structure cannot be also of the AF1 type reported for YMn_2 [23, 24].

3.3. Magnetic and nuclear structures in $Ho(Mn_{0.95}Al_{0.05})_2$ and $HoMn_2$

The two samples with $x = 0.0$ and 0.05 show similar heterogeneity as $Ho(Mn_{0.9}Al_{0.1})_2$ does. The magnetic structures observed in these samples resemble those identified in $Ho(Mn_{0.9}Al_{0.1})_2$. Some differences concern the incommensurate magnetic structure. In $Ho(Mn_{0.95}Al_{0.05})_2$ the incommensurate structure has a wave vector $\boldsymbol{k} = [0.210(5), 0.210(5), 0.089(8)]$ and arises in the crystallographic phase with the larger lattice parameter. The volume content of the phases with the smaller and larger lattice parameter was found to be 47.9% and 52.1%, respectively. The lower intensity of the '0' satellite in $Ho(Mn_{0.95}Al_{0.05})_2$ (see figure 1) is likely due to a smaller value of the magnetic moments in the incommensurate structure.

A weak '0' satellite was also observed in the $HoMn_2$ sample (figure 1). Satellite 'A' can only be seen in the resulting pattern by summing up all the patterns collected below 25 K. The two-phase profile refinement of $HoMn_2$ shows a very small amount of the crystallographic phase with the larger lattice parameter (about 3.7%) to which the incommensurate magnetic phase should be ascribed. Hence, the incommensurate magnetic structure exists only in the small amount of the 'impurity' phase with the same C15 cubic structure as present in the total $HoMn_2$ sample. This circumstance can explain the low intensity of the '0' satellite. The satellite positions were calculated for the larger lattice parameter to give the wave vector $\boldsymbol{k} = [0.178, 0.178, 0.096]$. This value is close to those found for the other two samples. The temperature dependence of the magnetic contribution

to the nuclear reflections and the corresponding values of the sublattice magnetic moments of the as-cast $HoMn_2$ sample were in good agreement with the results of [11, 12, 14].

As in the case of $Ho(Mn_{0.9}Al_{0.1})_2$, the broad maxima were only observed in the neutron diffraction patterns of these samples at the positions which correspond to the Bragg reflections with half-integer indices.

4. Discussion

Depending on the sample preparation procedure, either a collinear ferrimagnetic structure with moments: $m_{Ho} = 8.12\ \mu_B$ and $m_{Mn} = -0.84\ \mu_B$ [12] or a spin-canted ferrimagnetic structure with $m_{Ho} = 7.8\ \mu_B$ and $m_{Mn} = -0.6\ \mu_B$ in one out of four Mn sites [14] was observed earlier in the cubic $HoMn_2$ compounds.

The as-cast $Ho(Mn_{1-x}Al_x)_2$ samples studied in this work have inhomogeneous (two phase) microstructure each showing different magnetic ordering. In the as-cast $HoMn_2$ sample, no MnO-type antiferromagnetic structure was stabilized. Instead, antiferromagnetic short range correlations appear based on the AF2-type structure. Note that broad diffuse 'maxima' with half-integer indices associated with 4f-correlations based on the AF2 structure were observed in the $Ho_{1-x}Y_xMn_2$ system at $0.35 < x < 0.65$ [16]. As in the case of the as-cast samples, these correlations persist at temperatures much higher than T_C. In the $Ho(Mn_{1-x}Al_x)_2$ system, the correlations increase essentially with increasing Al concentration being more pronounced in the neutron diffraction patterns.

The wave vector of the incommensurate magnetic phase $\boldsymbol{k} \approx [0.18, 0.18, 0.08]$ is weakly dependent on x throughout the $Ho(Mn_{1-x}Al_x)_2$ system up to $x = 0.1$. The crystal phase with the smaller lattice parameter has much higher Curie temperature (about 100–120 K) than T_C of the collinear and AF2 phases. The lattice parameter of the crystal phase, to which the incommensurate structure belongs, lies within the narrow interval 7.49–7.52 Å that corresponds to the Mn–Mn spacing between 2.648 and 2.659 Å. It is hence lower than the critical value 2.663 Å reported for $(Ho, Y)Mn_2$ [16], above which an intrinsic Mn moment should appear. In contrast, the lattice parameter of the latter crystal phase changes substantially depending on the Al concentration (from 7.4585(3) Å in $HoMn_2$ to 7.5747(5) Å in $Ho(Mn_{0.9}Al_{0.1})_2$), again being still lower than the critical value a_c.

The high temperature heat treatment followed by quenching should provide a homogeneous microstructure of the samples. This procedure is however expected to dissolve the crystal phase which is responsible for the incommensurate magnetic structure. Some special studies concerning the preparation conditions are desirable in order to find out whether the incommensurate magnetic structure can exist in an isolated form in homogeneous samples. This magnetic structure can also be present in other RMn_2 compounds in which the Mn sublattice is in the NTP.

5. Concluding remarks

The magnetic structure of $HoMn_2$ as well as that of $HoMn_2$-based substituted compounds can be essentially different depending on sample preparation. The use of heterogeneous non-equilibrium samples makes it possible to find them in one sample material. Non-equilibrium as-cast samples of the $Ho(Mn_{1-x}Al_x)_2$ compounds show a number of magnetic structures, which can also be stabilized in undiluted $HoMn_2$: (i) collinear ferrimagnetic structure; (ii) AF2 MnO-type antiferromagnetic structure; (iii) incommensurate modulated magnetic structure and (iv) short range antiferromagnetic correlations based on the MnO-

type structure. Note that the incommensurate structure has a comparatively high ordering temperature; it was not observed in one sample material separately and arose in the non-equilibrium crystal phases only.

Acknowledgments

We are grateful to B E Kvyatkovsky and S V Sharygin for their assistance during the neutron diffraction experiments at the Gatchina diffractometer. The work was supported by RFBR (Pr. N-96-02-18673), INTAS (Pr. 096-0630) and the Russian Federal Foundation for Neutron Studies on Condensed Matter.

References

[1] Shiga M 1988 *Physica* B **149** 293
[2] Nakamura H, Wada H, Yoshimura K, Shiga M, Nakamura Y, Sabucri J and Komura Y 1988 *J. Phys. F: Met. Phys.* **18** 981
[3] Shiga M 1992 *J. Magn. Magn. Mater.* **129** 17
[4] De Teresa J M, Ibarra M R, Ritter C, Marquina C, Arnold Z and del Moral A 1995 *J. Phys.: Condens. Matter* **7** 5643
[5] Ritter C, Marquina C and Ibarra M R 1995 *J. Magn. Magn. Mater.* **151** 59
[6] De Teresa J M, Ritter C, Ibarra M R, Arnold Z, Marquina C and del Moral A 1996 *J. Phys.: Condens. Matter* **8** 8385
[7] Gaidukova I Yu, Dubenko I S and Markosyan A S 1985 *Fiz. Met. Metalloved.* **59** 300 (Engl. Transl. *Phys. Met. Metallogr.* **59** 79)
[8] Ibarra M R, Marquina C and del Moral A 1993 *Solid State Commun.* **87** 695
[9] Gaidukova I Yu, Kruglyashov S B, Markosyan A S, Levitin R Z, Pastushenkov Yu G and Snegirev V V 1983 *Zh. Eksp. Teor. Fiz.* **84** 1858 (Engl. Transl. *Sov. Phys.–JETP* **57** 1083)
[10] Ibarra M R, Garcia-Orza L and del Moral A 1992 *Solid State Commun.* **84** 785
[11] Chamberlain J 1977 *Physica* B **86–88** 138
[12] Hardman K, Rhyne J J, Malik S K and Wallace W 1982 *J. Appl. Phys.* **53** 1944
[13] Ritter C, Kilcoyne S H and Cywinsky R 1991 *J. Phys.: Condens. Matter* **3** 727
[14] Ritter C, Cywinsky R, Kilcoyne S H and Mondal S 1992 *J. Phys.: Condens. Matter* **4** 1559
[15] Brown P, Quladdiaf B, Ballou R, Deportes J and Markosyan A S 1992 *J. Phys.: Condens. Matter* **4** 1103
[16] Ritter C, Cywinski R and Kilcoyne S H 1994 *Z. Naturf.* a **50** 191
[17] Ritter C, Cywinsky R, Kilcoyne S H, Mondal S and Rainford B 1994 *Phys. Rev.* B **50** 9894
[18] Ritter C, Mondal S, Kilcoyne S H, Cywinski R and Rainford B 1992 *J. Magn. Magn. Mater.* **104–107** 1427
[19] Shiga M, Wada H, Yoshimura K and Nakamura Y 1987 *J. Phys. F: Met. Phys.* **17** 1781
[20] Rodriguez-Carvajal J 1996 *Program FULLPROF version of 1996* (Saclay: LLB CEA)
[21] Vochmyanin A P, Menshikov A Z and Pirigov A N 1994 *Fiz. Tverd. Tela* **36** 340 (in Russian)
[22] Thompson P, Cox D E J and Hastings B 1987 *J. Appl. Cryst.* **20** 79
[23] Cywinski R, Kilcoyne S H and Scott C 1991 *J. Phys.: Condens. Matter* **3** 6473
[24] Nakamura Y, Shiga M and Kawano S 1983 *Physica* B **120** 212